



Closer proximity of pre-treatment CD4⁺ T cells to CD8⁺ T cells favor response to neoadjuvant immunotherapy in patients with PD-L1 low-expressing non-small cell lung cancer

Liyang Yang^{1,2#}, Jiaxiao Geng^{2,3#}, Hao Yang^{3,4}, Miaoqing Zhao⁵, Hongtu Yuan⁵, Yushan Yan⁶, Li Wu⁶, Fanghan Cao³, Ligang Xing², Xiaorong Sun⁴

¹Shandong University Cancer Center, Shandong University, Jinan, China; ²Department of Radiation Oncology, Shandong Cancer Hospital and Institute, Shandong First Medical University, and Shandong Academy of Medical Sciences, Jinan, China; ³Department of Graduate, Shandong First Medical University and Shandong Academy of Medical Sciences, Jinan, China; ⁴Department of Nuclear Medicine, Shandong Cancer Hospital and Institute, Shandong First Medical University and Shandong Academy of Medical Sciences, Jinan, China; ⁵Department of Pathology, Shandong Cancer Hospital and Institute, Shandong First Medical University and Shandong Academy of Medical Sciences, Jinan, China; ⁶Department of Oncology, The Affiliated Hospital of Southwest Medical University, Southwest Medical University, Luzhou, China

Contributions: (I) Conceptualization and design: L Yang, X Sun; (II) Administrative support: M Zhao, H Yuan, L Xing, X Sun; (III) Provision of study materials or patients: L Yang, J Geng, H Yang, M Zhao, H Yuan, L Xing, Y Yan, L Wu; (IV) Collection and assembly of data: L Yang, J Geng, H Yang, Y Yan, L Wu; (V) Data analysis and interpretation: L Yang, J Geng, H Yang, Y Yan, L Wu; (VI) Manuscript writing: All authors; (VII) Final approval of manuscript: All authors.

[#]These authors contributed equally to this work as co-first authors.

Correspondence to: Xiaorong Sun, MD, PhD. Department of Nuclear Medicine, Shandong Cancer Hospital and Institute, Shandong First Medical University and Shandong Academy of Medical Sciences, No. 440, Jiyan Road, Huaiyin District, Jinan 250117, China. Email: xrsun@sdfmu.edu.cn.

Background: Neoadjuvant chemo-immunotherapy improves non-small cell lung cancer (NSCLC) outcomes, but remission rates vary, emphasizing the need for biomarkers. This study aimed to investigate the impact of the baseline intratumoral CD4⁺ T-cell-adjacent microenvironment on the efficacy of neoadjuvant immunotherapy in NSCLC and its correlation with hypoxia-inducible factor-1 α (HIF-1 α), microvessel density (MVD), and cancer-associated fibroblasts (CAFs).

Methods: Tumor samples from 49 NSCLC patients before neoadjuvant immunotherapy were retrospectively collected and subjected to multiplex immunohistochemistry staining (panel 1: DAPI/CK/CD4/CD8/CD68; Panel 2: DAPI/CK/CD4/HIF-1 α /CD31/ α -SMA) to characterize CD4⁺ T cells, CD8⁺ T cells CD68⁺ macrophages, HIF-1 α ⁺ cells, HIF-1 α ⁺CD4⁺ cells, MVD, and CAF. Mann-Whitney *U* test and receiver operating characteristic (ROC) curve were used to assess the relationship between the number and spatial distribution of each metric and the efficacy of the treatment, and Spearman's rank correlation was used to assess the correlation of each metric.

Results: In 49 NSCLC patients, responders (54.2%) and non-responders (45.8%). Single-indicator analysis revealed a positive correlation between high infiltration of CD8⁺ T cells in the stromal area and response to treatment in overall and programmed cell death-ligand 1 (PD-L1) low-expressing patients [CD8⁺ T (str) density: overall patient, 38 *vs.* 16, *P*=0.03; tumor proportion score (TPS) 1–49% subgroup, 37 *vs.* 14, *P*=0.04], with an area under curve (AUC) 0.684 and 0.746, respectively. CD4⁺ T cells combined with CD8⁺ T cells or CD68⁺ macrophages were analyzed and found to be more efficacious than CD4⁺T^{hi}CD8⁺T^{hi} compared to CD4⁺T^{lo}CD8⁺T^{lo} in patients with low expression of PD-L1 (*P*=0.03). Assessment of the nearest neighbor distance (NND) of CD4⁺ T cells and their adjacent cells revealed that the closer the CD4⁺ T cells and CD8⁺ T cells in the overall compartment, the better the efficacy in NSCLC patients, especially in patients with low PD-L1 expression [CD4⁺ T to CD8⁺ T (all) NND: overall patients, 34 *vs.* 47 μ m, *P*=0.03; TPS 1–49% subgroup, 34 *vs.* 69 μ m, *P*=0.006], and the AUC was 0.670 and 0.830, respectively. Notably, this favorable spatial interaction may not be dependent on direct contact between CD4⁺ T cells and CD8⁺ T cells within 10/20/30 μ m (*P*>0.05). Furthermore, in overall and PD-L1 low-expressing patients, the closer the

distance between CD4⁺ T cells and CD8⁺ T cells, the higher the MVD (overall patients, $r=-0.39$, $P=0.008$; TPS 1–49% subgroup, $r=-0.49$, $P=0.01$).

Conclusions: The baseline intratumoral CD4⁺ T-cell-adjacent microenvironment in NSCLC is associated with the efficacy of neoadjuvant immunotherapy for NSCLC, with the closer proximity of pre-treatment CD4⁺ T cells and CD8⁺ T cells, the better the treatment efficacy in NSCLC patients (even especially in the low-expressing PD-L1 population), and is associated with high MVD.

Keywords: Lung cancer; CD4⁺ T cells; spatial interaction; neoadjuvant immunotherapy; multiplex immunohistochemistry

Submitted Sep 25, 2024. Accepted for publication Feb 13, 2025. Published online Mar 26, 2025.

doi: 10.21037/tlcr-24-886

View this article at: <https://dx.doi.org/10.21037/tlcr-24-886>

Introduction

Non-small cell lung cancer (NSCLC) patients who receive neoadjuvant chemotherapy in conjunction with

immunotherapy exhibit a recurrence-free survival (RFS) rate of up to 60% at 4 years postoperatively (1). Moreover, a study indicated (2) that RFS is even more favorable among patients who achieve a major pathological response (MPR). However, approximately 50% of patients do not attain MPR following treatment (1). Therefore, it is essential to identify potential MPR beneficiaries to facilitate precise and individualized treatment strategies. Tumor mutation burden and programmed cell death 1/programmed cell death-ligand 1 (PD-1/PD-L1) expression (3–8), which are commonly employed as predictive markers in advanced stages, have proven to be inadequate in forecasting the efficacy of neoadjuvant immunotherapy. Thus, further exploration and discovery are essential to establish a precision immunotherapy framework guided by well-defined biomarkers.

CD4⁺ T cells in the tumor microenvironment are an indispensable component of current immunotherapy research. New evidence shows that CD4⁺ T cells can indirectly promote anti-tumor immunity by assisting in regulating the activation of CD8⁺ T cells (9–11), and can interact with effector macrophages to induce inflammatory cell death to inhibit immune escape, thereby indirectly killing tumor cells (12–15). However, the extent to which pre-existing CD4⁺ T cells in NSCLC tumors are in proximity to CD8⁺ T cells and CD68⁺ macrophages, and whether these cell-cell interactions influence the efficacy of neoadjuvant immunotherapy, remain unclear. Moreover, CD4⁺ T cells have been shown to be predominantly localized in mesenchymal rather than epithelial regions of tumors (12,16,17) yet the specific spatial domains where CD4⁺ T cells exert their indirect anti-tumor effects are not well understood.

In this study, we used multiplex immunohistochemistry

Highlight box

Key findings

- Revealing the spatial interactions of CD8⁺ T cells and CD68⁺ macrophages around CD4⁺ T cells at the baseline level.
- Clarifying that the proximity of CD4⁺ T cells to CD8⁺ T cells facilitated the efficacy of neoadjuvant immunotherapy.
- Discovering that the cellular interactions associated with the efficacy of the above immunotherapies may be influenced by the microvasculature in the tumor mesenchyme.

What is known and what is new?

- CD4⁺ T cells are primarily located in tumor stroma regions, but the specific spatial domains where CD4⁺ T cells exert their indirect anti-tumor effects are not well understood.
- Closer pre-treatment CD4⁺ and CD8⁺ T cells proximity correlates with better treatment outcomes in non-small cell lung cancer (NSCLC) patients, particularly within the low programmed cell death-ligand 1 (PD-L1) expression cohort and is associated with elevated microvessel density (MVD).

What is the implication, and what should change now?

- Baseline CD4⁺ T cells and CD8⁺ T cells proximity may be helpful in predicting the efficacy of neoadjuvant immunotherapy in NSCLC, but a multi-center and robust prediction model still needs to be constructed.
- The use of non-invasive and economical methods such as radiomics to predict the proximity of intratumoral CD4⁺ T cells and CD8⁺ T cells is expected to further enhance clinical translation and achieve large-scale application.
- Based on controlling tumor blood supply, improving tissue blood supply to the greatest extent may help promote intratumoral CD4⁺ T and CD8⁺ T contact with each other, thereby improving treatment efficacy.

(mIHC) to label neoadjuvant baseline CD4⁺ T cells and their adjacent microenvironment in NSCLC to evaluate the specific spatial distribution of CD4⁺ T cells and CD8⁺ T cells/CD68⁺ macrophages on the neoadjuvant impact of immunotherapy efficacy and analysis of its correlation with hypoxia-inducible factor-1 α (HIF-1 α), microvessel density (MVD), and cancer-associated fibroblasts (CAFs). We present this article in accordance with the STARD reporting checklist (available at <https://tldr.amegroups.com/article/view/10.21037/tldr-24-886/rc>).

Methods

Study population

In this study, a total of 49 patients diagnosed with NSCLC underwent radical surgery at Shandong Cancer Hospital and Institute. The enrollment criteria were as follows: (I) patients with clinical stage IIA–IIIB who received preoperative neoadjuvant PD-1 inhibitor therapy at Shandong Cancer Hospital between June 2021 and June 2023 [8th edition of the American Joint Committee on Cancer (AJCC)] (18); (II) a pathological diagnosis of either squamous lung cancer or lung adenocarcinoma; (III) availability of sufficient pre-treatment histological specimens; (IV) a clearly defined pre-treatment tumor proportion score (TPS); (V) wild-type status for epidermal growth factor receptor (EGFR); and (VI) a clear response to treatment, with patients achieving a major pathological response (MPR), defined as less than 10% residual viable tumor cells, categorized as responders (19), while those not meeting this criterion were classified as non-responders. The exclusion criteria included: (I) the presence of other concomitant malignant tumors; (II) a history of autoimmune disease; (III) incomplete clinical data; and (IV) inadequate specimens. The study was conducted in accordance with the Declaration of Helsinki (as revised in 2013). This study received approval from the Ethical Review Committee of Shandong Cancer Hospital and Institute (SDTHEC 2023003055). Given that this was a retrospective study, patient informed consent was not required. This research was partitioned into two cohorts: the responders group and the non-responders group. Individuals attaining an MPR were designated as responders, whereas the rest were classified as non-responders.

mIHC staining

Paraffin-embedded and formalin-fixed (FFPE) tumor

specimens before treatment were collected. Two panels were designed for mIHC staining of which panel 1 included DAPI, CK, CD4, CD8, and CD68, and panel 2 included DAPI, CK, CD4, HIF-1 α , CD31, and α -SMA. The mIHC staining procedure was as described above (20–24). Serial 3- μ m-thick sections were cut from FFPE and deparaffinized in xylene, then rehydrated and washed. Antigen retrieval was performed in heated tris-ethylenediamine tetra acetic acid (Tris-EDTA) (pH 9.0). Each section underwent several rounds of sequential staining, each containing a protein block followed by primary antibodies and corresponding secondary horseradish peroxidase-conjugated polymers. The slides were then incubated with Opal tyramine signal amplification (TSA) fluorescent dye diluted in amplification buffer. Tissue slides stained with TSA were counterstained with DAPI and mounted in antifade mounting medium. Comprehensive details on all primary antibodies and Opal used can be found in [Table S1](#). The Vectra Polaris scanner system and inForm software were used to scan stained slides. Raw multispectral images were used for algorithm development incorporating tissue segmentation, cell segmentation phenotyping tools, and spatial analysis.

Cell phenotype definition

The Vectra Polaris scanner system and inForm software were used to scan stained slides (25,26). Raw multispectral images were used for algorithm development incorporating tissue segmentation, cell segmentation phenotyping tools, and spatial analysis. For Panel 1, CD4⁺ CD8[−] CD68[−] CK[−] was used for indicating CD4⁺ T cells, CD4[−] CD8⁺ CD68[−] CK[−] for cytotoxic T cells, and CD4[−] CD8[−] CD68⁺ CK[−] for CD68⁺ macrophages. For Panel 2, CD4[−] HIF-1 α ⁺ CD31[−] α -SMA[−] CK[−] was used for indicating cells expressing HIF-1 α ⁺, CD4[−] HIF-1 α ⁺ CD31[−] α -SMA[−] CK[−] for indicating CD4⁺ T cells expressing HIF-1 α ⁺, CD4[−] HIF-1 α [−] CD31⁺ α -SMA[−] CK[−] for indicating MVD (27), and CD4[−] HIF-1 α [−] CD31[−] α -SMA⁺ CK[−] for CAF (28).

Machine learning-assisted multispectral image analysis

Apply bioinformatics tools to interpret the quantitative and spatial characteristics of CD4 by calculating cell counts delineated by different multi-marker phenotypes and the nuclear-to-nuclear Euclidean distance between any two cell types (16). Cell density was ascertained through the normalization of the respective cell counts in relation to the total cell counts (cell/1,000 cells) (29). Nearest neighbor

distance (NND) analysis was conducted by calculating the mean distance (micron) from each CD4⁺ T cell to its nearest CD8⁺ T or CD68⁺ macrophages (30). To analyze neighboring cells within a specific radius of CD4 using proximity, defined as the number of CD4⁺ T cells having at least one CD8⁺ T cell or CD68⁺ macrophage within 10/20/30 micron (26).

Statistical analysis

Statistical analysis was performed with GraphPad Prism (8.0) and R software (4.1.2). The Kolmogorov-Smirnov test was employed to verify the nonnormal distribution of parameters across all cell phenotypes. The Mann-Whitney *U* test was utilized for the analysis of parameters in two independent samples. Receiver operating characteristic (ROC) curves were used to predict accuracy, specificity, and sensitivity. Spearman rank correlation coefficient was utilized to access the correlation between immune cells and stromal cells. The results were considered statistically significant if two-sided *P* < 0.05.

Results

Patients clinicopathological characteristics

Forty-eight NSCLC patients receiving neoadjuvant immunotherapy were retrospectively included. The baseline characteristics of the patients are shown in Table 1, including information on age, gender, smoking index, tumor location, clinical stage, histological type, Karnofsky performance status (KPS) score, and TPS score. After treatment 45.8% (22/48) of patients were non-responders and 54.2% (26/48) were responders, with balanced clinicopathologic information between patients in the non-responder and responder groups. The study flowchart is illustrated in Figure 1.

High pre-treatment CD8⁺ T cell density in tumor stroma correlates with positive response in overall and PD-L1 low-expression subgroups

To investigate the expression levels of CD4⁺ T cells, CD8⁺ T cells, and CD68⁺ macrophages in different regions of tumors from NSCLC patients prior to receiving neoadjuvant immunotherapy, we performed mIHC staining (DAPI/CK/CD4/CD8/CD68). We categorized the tissue regions based on CK expression into epithelial (CK⁺) and stromal (CK⁻) areas (Figure 2A). Representative images of

CD4⁺ T cells, CD8⁺ T cells, and CD68⁺ macrophages are shown in Figure 2B. The differences in the cell densities per thousand cells between the responding and non-responding groups are summarized in Table S2. In the overall patient population, there were no statistically significant differences in the densities of CD4⁺ T cells and CD68⁺ macrophages between the responders and non-responders across the overall, epithelial, or stromal regions. However, the infiltration of CD8⁺ T cells was significantly higher in the stromal area of responding patients [response *vs.* non-response: CD8⁺ T (str): 38 [10, 61] *vs.* 16 [6, 28], *P*=0.03] (Figure 2C). The ROC curve analysis indicated an area under the curve (AUC) of 0.684, with a specificity of 0.538 and sensitivity of 0.733 (Figure 2C).

Subsequently, we conducted a subgroup analysis based on TPS. Among the patients with PD-L1 negative expression (TPS <1%), there was only < one case (no subgroup analysis was performed); in the PD-L1 low expression group (TPS 1–49%), there were 26 patients, with 11 responders and 15 non-responders. In the PD-L1 high expression group (TPS ≥50%), there were 21 patients, with 21 responders and 7 non-responders. Results indicated that in PD-L1 low-expression NSCLC patients, the differences in tumor-infiltrating cells between responders and non-responders mirrored those observed in the overall patient cohort (Figure 2C; Table S2), showing higher levels of CD8⁺ T cells in both overall and stromal regions, which correlated with better treatment responses {CD8⁺ T (all): 33 [17, 63] *vs.* 14 [5, 20], *P*=0.045; CD8⁺ T (str): 37 [18, 50] *vs.* 14 [6, 25], *P*=0.04} (Figure 2D, 2E). The AUC, specificity, and sensitivity for CD8⁺ T cells in the overall region were 0.733, 0.727, and 0.800, respectively (Figure 2D), while in the stromal region, they were 0.746, 0.636, and 0.867 (Figure 2E). In contrast, no significant differences in cell infiltration levels were observed within the PD-L1 high expression group (Table S2).

Baseline CD4⁺T^{hi}CD8⁺T^{hi} in the overall compartment favors treatment response in patients with low PD-L1 expression

We further categorized patients based on the median expression levels of CD4⁺ T cells, CD8⁺ T cells, or CD68⁺ macrophages into high and low expression groups. We assessed the impact of CD4⁺ T cells combined with CD8⁺ T cells (CD4⁺T^{hi}CD8⁺T^{hi}/CD4⁺T^{hi}CD8⁺T^{lo}/CD4⁺T^{lo}CD8⁺T^{hi}/CD4⁺T^{lo}CD8⁺T^{lo}) and CD4⁺ T cells combined with CD68⁺ macrophages (CD4⁺T^{hi}CD68⁺macrophage^{hi}/

Table 1 Baseline characteristics of 48 patients with non-small cell lung cancer who received neoadjuvant immunotherapy

Characteristic	Overall [n=48 (100%)]	Non-response [n=22 (45.8%)]	Response [n=26 (54.2%)]	P
Age (years)				>0.99
≤65	25 (52.1)	11 (50.0)	14 (53.8)	
>65	23 (47.9)	11 (50.0)	12 (46.2)	
Gender				0.22
Male	41 (85.4)	17 (77.3)	24 (92.3)	
Female	7 (15.6)	5 (22.7)	2 (7.7)	
Smoking index [†]				0.77
≤400	18 (37.5)	9 (40.9)	9 (34.6)	
>400	30 (62.5)	13 (59.1)	17 (65.4)	
Tumor location				0.78
Peripheral	25 (52.1)	12 (54.5)	13 (50.0)	
Central	23 (47.9)	10 (45.5)	13 (50.0)	
cTNM stage AJCC 8th				0.61
IIA	2 (4.2)	0 (0.0)	2 (7.7)	
IIB	10 (20.8)	4 (18.2)	6 (23.1)	
IIIA	22 (45.8)	12 (54.5)	10 (38.5)	
IIIB	14 (29.2)	6 (27.3)	8 (30.8)	
Histology				0.08
Lung squamous cell carcinoma	37 (77.1)	14 (63.6)	23 (88.5)	
Lung adenocarcinoma	11 (22.9)	8 (36.4)	3 (11.5)	
Karnofsky performance status				0.89
80	11 (22.9)	6 (27.3)	5 (19.2)	
90	34 (70.8)	15 (68.2)	19 (73.1)	
100	3 (6.2)	1 (4.5)	2 (7.7)	
Tumor proportion score				0.11
<1%	1 (2.1)	0 (0.0)	1 (3.8)	
1–49%	26 (54.2)	15 (68.2)	11 (42.3)	
≥50%	21 (43.8)	7 (31.8)	14 (53.8)	
EGFR mutation status				NA
Wild	48 (100.0)	22 (100.0)	26 (100.0)	
Mutant	0 (0.0)	0 (0.0)	0 (0.0)	
ICI treatment				0.59
Anti-PD-L1	3 (6.2)	2 (9.1)	1 (3.8)	
Anti-PD-1	45 (93.8)	20 (90.9)	25 (96.2)	

[†], smoking index = smoking time (years) × number of cigarettes smoked per year (cigarettes). AJCC, American Joint Committee on Cancer; cTNM, clinical tumor-node-metastasis; EGFR, epidermal growth factor receptor; ICI, immune checkpoint inhibitor; NA, not applicable; PD-1, programmed cell death protein 1; PD-L1, programmed cell death-ligand 1.

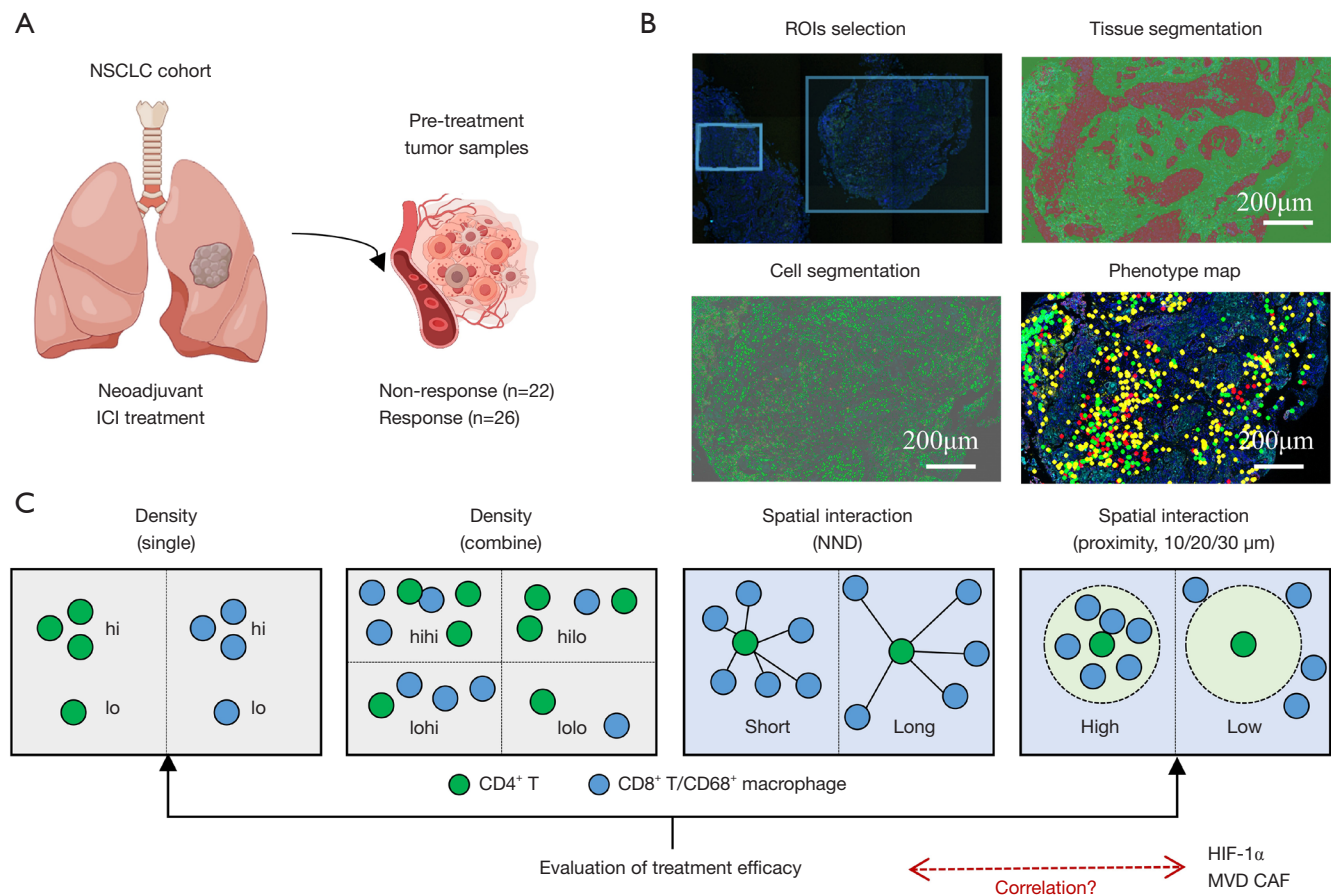


Figure 1 Identification and characterization of tumor microenvironment in NSCLC. (A) Cohorts and samples. (B) mIHC staining was used to characterize immune indicators and select the ROIs and proceed with tissue segmentation, cell segmentation, and Phenotype and identification, and the boxes represent ROIs. (C) Overview of the analysis variables. CAF, cancer-associated fibroblast; HIF-1 α , hypoxia-inducible factor 1 α ; ICI, immune checkpoint inhibitor; mIHC, multiplex immunohistochemistry; MVD, microvessel density; NND, nearest neighbor distance; NSCLC, non-small cell lung cancer; ROI, region of interest.

$CD4^+T^{hi}CD68^+macrophage^{lo}/CD4^+T^{lo}CD68^+macrophage^{hi}/CD4^+T^{lo}CD68^+macrophage^{lo}$) on treatment efficacy in NSCLC patients undergoing neoadjuvant therapy. In both overall and PD-L1 high expression NSCLC patient groups, no significant results were found. Conversely, in the overall region of PD-L1 low expression patients, the response was better for those with $CD4^+T^{hi}CD8^+T^{hi}$ compared to $CD4^+T^{lo}CD8^+T^{lo}$ ($P=0.03$) (Table S3).

Proximity between $CD4^+$ T and $CD8^+$ T cells in the stroma affects treatment response in PD-L1 low expression patients

We also explored the impact of the NNDs between $CD4^+$ T cells and $CD8^+$ T cells, as well as $CD68^+$ macrophages, on

the efficacy of neoadjuvant immunotherapy for NSCLC. In the overall patient population, treatment efficacy depended on the distance between $CD4^+$ T cells and $CD68^+$ macrophages (Table S4). Shorter distances between $CD4^+$ T and $CD8^+$ T cells correlated with better treatment outcomes [34 [22, 51] vs. 47 [33, 86] μm , $P=0.03$], with an AUC of 0.670, specificity of 0.952, and sensitivity of 0.417.

Similar results were observed in PD-L1 low expression patients [34 [24, 39] vs. 69 [39, 101] μm , $P=0.006$] (Figure 3A,3B), with an AUC of 0.830, specificity of 0.533, and sensitivity of 1.000 (Figure 3C). Furthermore, this phenomenon was noted in the tumor stroma but not in the epithelial region [39 [27, 39] vs. 69 [40, 125] μm ,

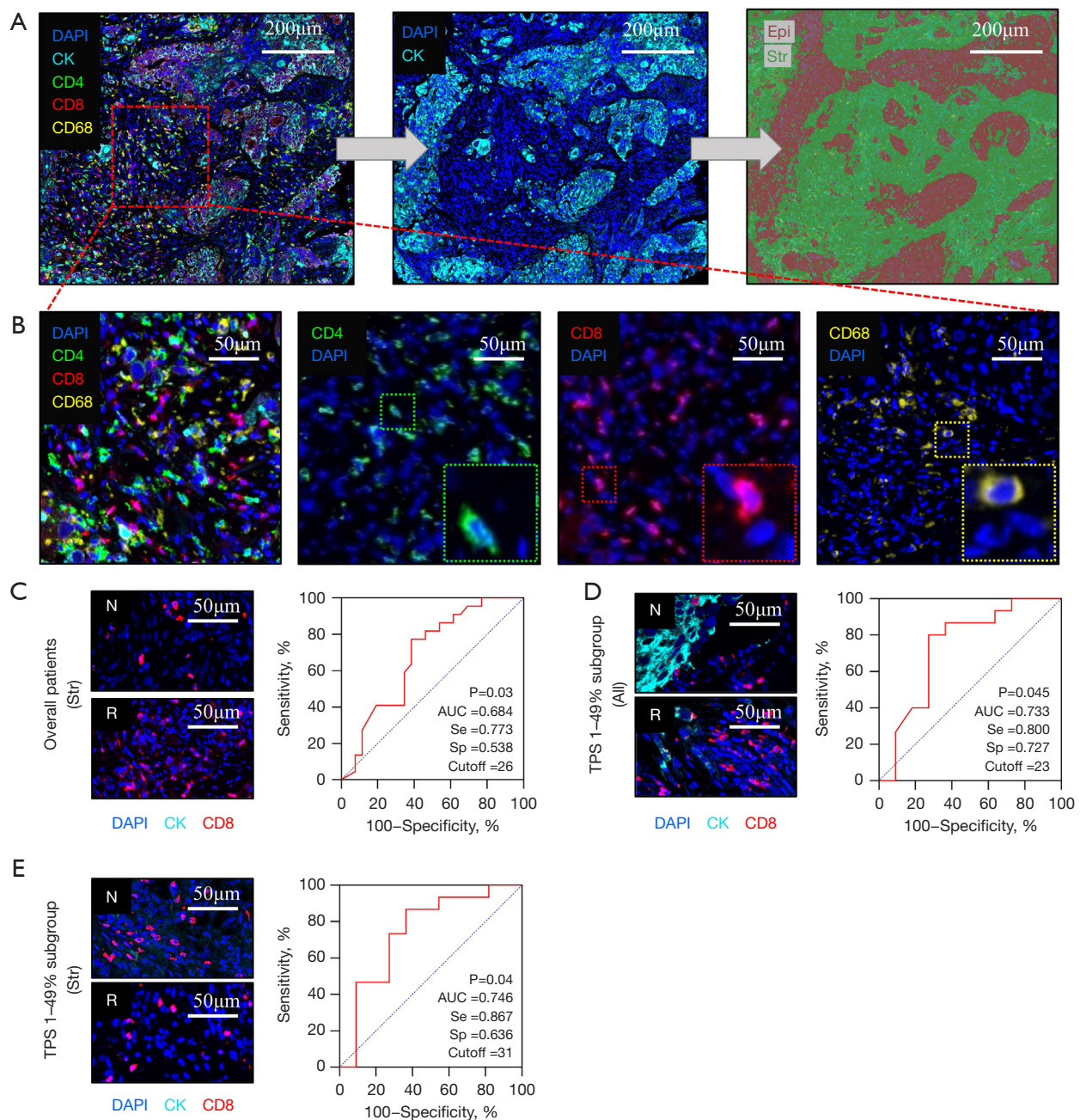


Figure 2 mIHC characterization of the impact of CD4⁺ T cells, CD8⁺ T cells, and CD68⁺ macrophage densities in different regions of NSCLC patients on the efficacy of neoadjuvant immunotherapy. (A) Representative mIHC images from panel 1 and tissue segmentation images, where CK⁺ indicates the epithelial compartment, and CK⁻ indicates the stromal compartment. Epi, epithelial compartment. Str, stromal compartment, and the boxes represent enlarged immune indicators. (B) Representative images of CD4⁺ T cells, CD8⁺ T cells, and CD68⁺ macrophages, and the boxes represent enlarged immune indicators. (C) Differences in CD8⁺ T cell density between responders and non-responders in the stromal compartment of all patients (left), and the corresponding ROC curve (right). (D) Differences in CD8⁺ T cell density between responders and non-responders in the total compartment of PD-L1 low-expressing patients (left), and the corresponding ROC curve (right). (E) Differences in CD8⁺ T cell density between responders and non-responders in the stromal compartment of PD-L1 low-expressing patients (left), and the corresponding ROC curve (right). AUC, area under the curve; DAPI, 4',6-diamidino-2-phenylindole; mIHC, multiplex immunohistochemistry; N, non-response; NSCLC, non-small cell lung cancer; PD-L1, programmed cell death-ligand 1; R, response; ROC, receiver operating characteristic; Se, sensitivity; Sp, specificity; TPS, tumor proportion score.

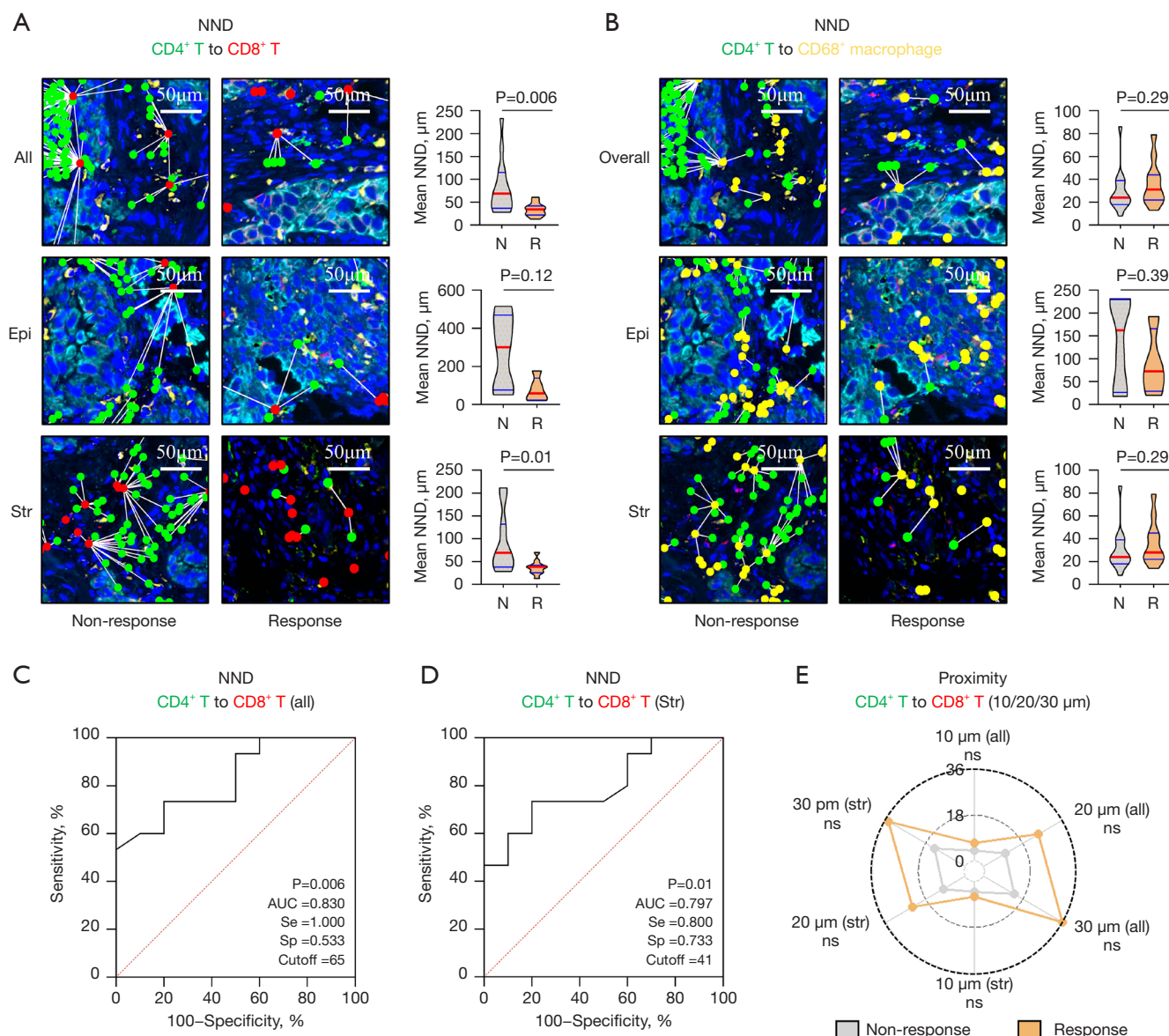


Figure 3 The impact of spatial interactions between CD4⁺ T cells and CD8⁺ T cells, as well as CD68⁺ macrophages, on the efficacy of neoadjuvant immunotherapy in PD-L1 low-expressing NSCLC patients. (A) mIHC staining was used to analyze differences in the NND between CD4⁺ T cells and CD8⁺ T cells in different compartments and representative images (left). (B) mIHC staining was used to analyze differences in the NND between CD4⁺ T cells and CD68⁺ macrophages in different compartments and representative images (left). (C) ROC curve of the NND between CD4⁺ T cells and CD8⁺ T cells in the total compartment in relation to treatment efficacy. (D) ROC curve of the NND between CD4⁺ T cells and CD8⁺ T cells in the stromal compartment in relation to treatment efficacy. (E) Radar chart showing the relationship between the proximity (10/20/30 μm) of CD4⁺ T cells and CD8⁺ T cells and the efficacy of neoadjuvant immunotherapy in NSCLC patients. AUC, area under the curve; DAPI, 4',6-diamidino-2-phenylindole; Epi, epithelial compartment; mIHC, multiplex immunohistochemistry; N, non-response; NND, nearest neighbor distance; NSCLC, non-small cell lung cancer; PD-L1, programmed cell death-ligand 1; R, response; ROC, receiver operating characteristic; Se, sensitivity; Sp, specificity; Str, stromal compartment, and the boxes represent enlarged immune indicators.

$P=0.01$ }, with AUC values of 0.797, specificity of 0.733, and sensitivity of 0.800 (Figure 3D). The AUC values for the interaction between CD4⁺ and CD8⁺ T cells were consistently higher than those for CD8⁺ T cell infiltration alone, indicating superior predictive efficacy of CD4⁺-CD8⁺ T cell proximity (Figures 2D, 2E, 3C, 3D). No treatment response-related immune indicators were found in the PD-L1 high expression patient group. In patients with NSCLC, neither the infiltration of CD8⁺ T cells nor the NNDs between CD4⁺ and CD8⁺ T cells exhibited statistically significant differences between the PD-L1 low-expression and high-expression cohorts (Table S5).

Theoretically, CD4⁺ T cells and CD8⁺ T cells may interact through both direct and indirect mechanisms. In the aforementioned NND analysis, we observed that closer proximity between CD4⁺ T and CD8⁺ T cells enhanced the efficacy of neoadjuvant immunotherapy, with an effective distance exceeding the previously reported direct contact distance of 30 μm (29,31-33). This suggests that indirect interactions may play a predominant role between CD4⁺ T and CD8⁺ T cells.

No correlation between CD4⁺ T cell proximity to CD8⁺ T cells/CD68⁺ macrophages and treatment efficacy

To test this hypothesis, we further analyzed the proximity of CD4⁺ T cells to CD8⁺ T cells and CD68⁺ macrophages at different distances (10/20/30 μm) and its effect on treatment efficacy. Consistent with expectations, there was no correlation between CD4⁺ T cells and adjacent cells at 10/20/30 μm distances regarding treatment response, whether in the overall (Table S6), PD-L1 low expression (Figure 3E; Table S6), or PD-L1 high expression groups (Table S6). In summary, our findings support the notion that CD4⁺ T cells exert their physiological effects on CD8⁺ T cells without requiring direct contact.

Shortened distances between CD4⁺ T and CD8⁺ T cells correlate with high MVD density

To further investigate the correlation between HIF-1 α , MVD, CAF, and the proximity of CD4⁺ T cells to CD8⁺ T cells, we performed mIHC staining on the stromal components of the tumor microenvironment (DAPI/CK/CD4/HIF-1 α /CD31/ α -SMA) (Figure 4A). The results indicated that in the overall patient population, the NND between CD4⁺ T and CD8⁺ T cells negatively correlated with MVD in the overall region ($r=-0.39$, $P=0.008$)

(Figure S1A), suggesting that closer distances corresponded with higher MVD density. Interestingly, no correlation between the NND of CD4⁺ T and CD8⁺ T cells and MVD was found in the responding patient group ($r=-0.13$, $P=0.54$) (Figure S1B). However, a stronger correlation was observed among non-MPR patients ($r=-0.61$, $P=0.004$) (Figure S1C). Notably, this correlation was particularly significant in PD-L1 low expression patients ($r=-0.49$, $P=0.01$; response, $r=0.09$, $P=0.80$; non-response, $r=-0.61$, $P=0.02$) (Figure 4B, 4C; Figure S1D).

Discussion

Our study aims to elucidate the spatial characteristics of CD4⁺ T cells and their interactions with CD8⁺ T cells and CD68⁺ macrophages, as well as how these interactions may potentially influence the efficacy of neoadjuvant immunotherapy in patients with NSCLC. By employing mIHC, we are able to intricately map the tumor microenvironment and highlight the significance of identifying key cellular interactions.

Effector CD8⁺ T cells have been suggested as possible tumor-specific cells in immunotherapy (34-37), and our results indicate that there is a significant correlation between high CD8⁺ T cells densities in the tumor stroma prior to treatment and the response to treatment, especially in patients with low PD-L1 expression. However, the conventional view suggests that CD8⁺ T cell accumulation in the stroma rather than the epithelium is typically associated with 'immune exclusion', which is related to tumor immune evasion (38). The discrepancy may stem from our observation that CD8⁺ T cells are not exclusively localized in the stromal region but are also distributed within the tumor parenchyma, suggesting that this phenomenon may not entirely equate to immune exclusion. Current research indicates that tumor-infiltrating lymphocytes (TILs) exhibit heterogeneous distribution in NSCLC tissues. Notably, in pre-treatment specimens from NSCLC patients receiving immune checkpoint inhibitor (ICI) therapy, TILs were preferentially distributed in the stromal areas surrounding tumor cell nests, with the CD8⁺ T cell subset being the most abundant. Increased CD8⁺ T cell density in the stroma was significantly associated with prolonged survival (39,40). Furthermore, in early-stage endometrial cancer samples, high TIL infiltration in the tumor stromal region was associated with favorable patient prognosis (41). These findings are consistent with our results (17,42). To further elucidate this mechanism, we conducted an in-depth analysis

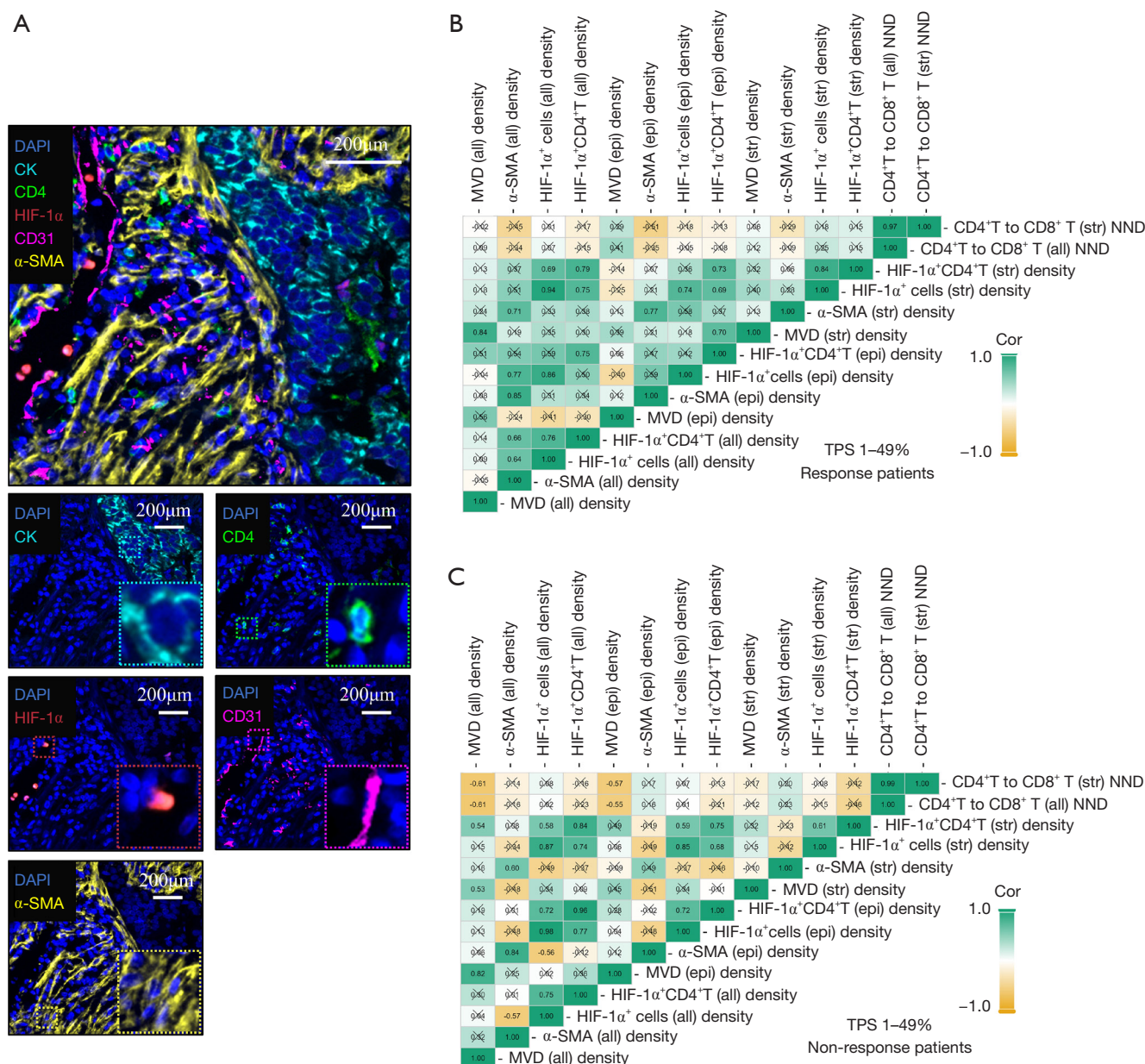


Figure 4 A shorter NND between CD4⁺ T cells and CD8⁺ T cells is positively correlated with MVD. (A) A multispectral mixed image of panel 2 from the mIHC showing representative illustrations of tumor cells, CD4⁺ T cells, HIF-1 α -expressing cells, MVD, and CAFs, and the boxes represent enlarged immune indicators. (B) Correlation heatmap of various immune markers within different compartments in PD-L1 low-expressing responders. (C) Correlation heatmap of various immune markers within different compartments in PD-L1 low-expressing non-responders. CAF, cancer-associated fibroblast; DAPI, 4',6-diamidino-2-phenylindole; HIF-1 α , hypoxia-inducible factor-1 α ; mIHC, multiplex immunohistochemistry; MVD, microvascular density; NND, nearest neighbor distance; PD-L1, programmed cell death-ligand 1; SMA, smooth muscle actin; TPS, tumor proportion score.

of immune cell interactions. Our results revealed significant co-enrichment of CD4⁺ T cells in stromal regions with high CD8⁺ T cell infiltration. This finding suggests that

CD8⁺ T cells in the stromal region may exert their anti-tumor effects through interactions with CD4⁺ T cells. These observations suggest that the stromal infiltration of

CD8⁺ T cells may not always represent immune exclusion but could instead reflect a functional immune response that contributes to therapeutic efficacy. In summary, while the concept of immune exclusion traditionally carries a negative connotation, our findings challenge this paradigm in the context of neoadjuvant chemo-immunotherapy for NSCLC. The stromal infiltration of CD8⁺ T cells appears to be a positive indicator of therapeutic response, underscoring the importance of considering both the spatial distribution and interactions between immune cells in evaluating immunotherapy outcomes.

However, the densities of CD4⁺ T cells and CD68⁺ macrophages did not show significant differences between responders and non-responders, suggesting that these cells themselves may not be reliable predictive markers of response to treatment. CD4⁺ T cells enhance the antitumor immune response of CD8⁺ T cells primarily by secreting interferon-gamma (IFN- γ) (15,43-45). Our analysis indicates that the proximity between CD4⁺ T cells and CD8⁺ T cells in the stromal region is a key factor influencing treatment efficacy. This proximity may facilitate indirect interactions, thereby enhancing the anti-tumor immune response. Furthermore, we found that the number of CD8⁺ T cells within 30 μ m of CD4⁺ T cells is not correlated with the efficacy of neoadjuvant immunotherapy. Since 30 micrometers is the two-dimensional physical distance supported by previous literature for direct cell-cell interactions (33,46), this also indirectly suggests that in neoadjuvant immunotherapy, CD4⁺ T cells may promote anti-tumor immunity of CD8⁺ T cells through indirect mechanisms.

Stratified analyses revealed this favorable spatial interplay only in the group of patients with low PD-L1 expression, while the lack of significant treatment-related immune indicators in the group with high PD-L1 expression underscores the complexity of the immune environment. Research has shown that intertumoral exhausted CD4⁺ T cells are involved in the response to ICI therapy. Specifically, the blockade of PD-1 on PD-1^{hi}CD39⁺CD4⁺ T cells can promote the proliferation of specific autologous CD8⁺ T cells (47). However, it remains unclear whether a substantial presence of these specific PD-1^{hi}CD39⁺CD4⁺ T cells exists in patients with low PD-L1 expression. This uncertainty presents an intriguing avenue for future exploration. Moving forward, we plan to further delineate the functions of CD4⁺ T cells, including traditional CD4⁺ T cells, regulatory CD4⁺ T cells, and exhausted CD4⁺ T cells. Our aim is to determine whether the interaction between

CD4⁺ T cells in specific functional states and CD8⁺ T cells can enhance the ICI therapy response in patients with low PD-L1 expression. This insight could potentially guide stratified treatment approaches.

The relationship between the proximity of CD4⁺ T cells and CD8⁺ T cells and high MVD provides additional insights into the dynamics of the tumor microenvironment. The negative correlation between the closeness of CD4⁺ and CD8⁺ T cells and MVD suggests that more vascularized tumor stroma may facilitate tighter cellular interactions, thereby enhancing the immune response. Basic research indicates that endothelial cells in the tumor microenvironment recruit immune cell infiltration by secreting chemokines (48-50). Meanwhile, specific functional CD8⁺ T cells can secrete vascular endothelial growth factor, and CD4⁺ T cells can promote angiogenesis through the secretion of cytokines such as IL-17 (51), further supporting anti-tumor immune responses (52). Therefore, improving blood supply in the tumor stroma may enhance CD4⁺ T and CD8⁺ T cell interactions, thereby increasing the efficacy of immunotherapy. However, it is well known that vascular abundance can be a double-edged sword for tumor tissues: while increased blood supply may facilitate immune cell infiltration, it can also create favorable conditions for tumor cell proliferation. Thus, ensuring the delivery of immune cells while controlling the blood supply to tumor cells presents a significant challenge. Notably, this correlation is more pronounced in non-responders, suggesting that other factors may modulate this relationship among responders.

There are several limitations in this study. First, the sample size is relatively small, necessitating validation through larger multicenter cohorts to construct a more stable and reliable predictive model. Second, we did not further explore which specific functions of CD4⁺ T cells and CD8⁺ T cells are most conducive to the neoadjuvant therapy response, a topic that requires future investigation. Additionally, we did not delve into the precise mechanisms underlying the interactions between CD4⁺ and CD8⁺ T cells. Although we observed that their spatial proximity may be related to vascularization, this was not confirmed in basic research, potentially limiting our understanding of the deeper biological mechanisms behind treatment response. Moreover, the interactions between these cells could be influenced by various factors, including other immune cell types, cytokines, and metabolic products, all of which warrant further exploration in future studies.

Conclusions

Our study highlights although the therapeutic efficacy of chemo-immunotherapy in the patients with low PD-L1 expression is generally inferior to that in the patients with high PD-L1 expression, the patients with proximity between CD4⁺ and CD8⁺ T cells can benefit from chemo-immunotherapy even their PD-L1 expression is low. These findings provide new insights into personalized stratification for guiding immunotherapy strategies. Future research should focus on elucidating the mechanisms behind these interactions to refine and enhance immunotherapy approaches.

Acknowledgments

None.

Footnote

Reporting Checklist: The authors have completed the STARD reporting checklist. Available at <https://tldr.amegroups.com/article/view/10.21037/tldr-24-886/rc>

Data Sharing Statement: Available at <https://tldr.amegroups.com/article/view/10.21037/tldr-24-886/dss>

Peer Review File: Available at <https://tldr.amegroups.com/article/view/10.21037/tldr-24-886/prf>

Funding: This work was supported by grants from the National Natural Science Foundation of China (Nos. 82373424, 82172866, 82071035, 82371165), the Shandong Provincial Natural Science Foundation (No. ZR2021LZL005) and the Department of Science & Technology of Shandong Province (No. 2021CXGC011102).

Conflicts of Interest: All authors have completed the ICMJE uniform disclosure form (available at <https://tldr.amegroups.com/article/view/10.21037/tldr-24-886/coif>). The authors have no conflicts of interest to declare.

Ethical Statement: The authors are accountable for all aspects of the work in ensuring that questions related to the accuracy or integrity of any part of the work are appropriately investigated and resolved. The study was conducted in accordance with the Declaration of Helsinki (as revised in 2013). This study received approval from the

Ethical Review Committee of Shandong Cancer Hospital and Institute (SDTHEC 2023003055). Given that this was a retrospective study, patient informed consent was not required.

Open Access Statement: This is an Open Access article distributed in accordance with the Creative Commons Attribution-NonCommercial-NoDerivs 4.0 International License (CC BY-NC-ND 4.0), which permits the non-commercial replication and distribution of the article with the strict proviso that no changes or edits are made and the original work is properly cited (including links to both the formal publication through the relevant DOI and the license). See: <https://creativecommons.org/licenses/by-nc-nd/4.0/>.

References

1. Spicer J, Girard N, Provencio M, et al. Neoadjuvant nivolumab (NIVO)+ chemotherapy (chemo) vs chemo in patients (pts) with resectable NSCLC: 4-year update from Check-Mate 816. American Society of Clinical Oncology 2024;42:LB8010.
2. Carbone D, Waqar S, Chait J, et al. 145MO Updated survival, efficacy and safety of adjuvant (adj) atezolizumab (atezo) after neoadjuvant (neoadj) atezo in the phase II LCMC3 study. J Thorac Oncol 2023;18:S90-S1.
3. Deng H, Zhao Y, Cai X, et al. PD-L1 expression and Tumor mutation burden as Pathological response biomarkers of Neoadjuvant immunotherapy for Early-stage Non-small cell lung cancer: A systematic review and meta-analysis. Crit Rev Oncol Hematol 2022;170:103582.
4. Zhang F, Guo W, Zhou B, et al. Three-Year Follow-Up of Neoadjuvant Programmed Cell Death Protein-1 Inhibitor (Sintilimab) in NSCLC. J Thorac Oncol 2022;17:909-20.
5. Ricciuti B, Elkrif A, Alessi J, et al. Three-year outcomes and correlative analyses in patients with non-small cell lung cancer (NSCLC) and a very high PD-L1 tumor proportion score (TPS) ≥ 90% treated with first-line pembrolizumab. American Society of Clinical Oncology;2022;40:9043.
6. Özgüroğlu M, Kilickap S, Sezer A, et al. First-line cemiplimab monotherapy and continued cemiplimab beyond progression plus chemotherapy for advanced non-small-cell lung cancer with PD-L1 50% or more (EMPOWER-Lung 1): 35-month follow-up from a multicentre, open-label, randomised, phase 3 trial. Lancet Oncol 2023;24:989-1001.

7. Gadgeel S, Rodríguez-Abreu D, Halmos B, et al. OA14. 05 5-year survival of pembrolizumab plus chemotherapy for metastatic NSCLC with PD-L1 tumor proportion score < 1%. *J Thorac Oncol* 2023;18:S77-S78.
8. Provencio M, Nadal E, González-Larriba JL, et al. Perioperative Nivolumab and Chemotherapy in Stage III Non-Small-Cell Lung Cancer. *N Engl J Med* 2023;389:504-13.
9. Wei W, Su Y. Function of CD8(+), conventional CD4(+), and regulatory CD4(+) T cell identification in lung cancer. *Comput Biol Med* 2023;160:106933.
10. van der Leun AM, Thommen DS, Schumacher TN. CD8(+) T cell states in human cancer: insights from single-cell analysis. *Nat Rev Cancer* 2020;20:218-32.
11. Ben Khelil M, Godet Y, Abdeljaoued S, et al. Harnessing Antitumor CD4(+) T Cells for Cancer Immunotherapy. *Cancers (Basel)* 2022;14:260.
12. Kruse B, Buzzai AC, Shridhar N, et al. CD4+ T cell-induced inflammatory cell death controls immune-evasive tumours. *Nature* 2023;618:1033-40.
13. Speiser DE, Chijioke O, Schaeuble K, et al. CD4(+) T cells in cancer. *Nat Cancer* 2023;4:317-29.
14. Boulch M, Cazaux M, Cuffel A, et al. Tumor-intrinsic sensitivity to the pro-apoptotic effects of IFN- γ is a major determinant of CD4(+) CAR T-cell antitumor activity. *Nat Cancer* 2023;4:968-83.
15. Haabeth OA, Tveita AA, Fauskanger M, et al. How Do CD4(+) T Cells Detect and Eliminate Tumor Cells That Either Lack or Express MHC Class II Molecules? *Front Immunol* 2014;5:174.
16. Cai S, Zhao M, Yang G, et al. Modified spatial architecture of regulatory T cells after neoadjuvant chemotherapy in non-small cell lung cancer patients. *Int Immunopharmacol* 2024;137:112434.
17. Yang G, Cai S, Hu M, et al. Functional status and spatial architecture of tumor-infiltrating CD8+ T cells are associated with lymph node metastases in non-small cell lung cancer. *J Transl Med* 2023;21:320.
18. Goldstraw P, Chansky K, Crowley J, et al. The IASLC Lung Cancer Staging Project: Proposals for Revision of the TNM Stage Groupings in the Forthcoming (Eighth) Edition of the TNM Classification for Lung Cancer. *J Thorac Oncol* 2016;11:39-51.
19. Forde PM, Chaft JE, Smith KN, et al. Neoadjuvant PD-1 Blockade in Resectable Lung Cancer. *N Engl J Med* 2018;378:1976-86.
20. Corgnac S, Malenica I, Mezquita L, et al. CD103(+) CD8(+) T(RM) Cells Accumulate in Tumors of Anti-PD-1-Responder Lung Cancer Patients and Are Tumor-Reactive Lymphocytes Enriched with Tc17. *Cell Rep Med* 2020;1:100127.
21. Jahangir CA, Page DB, Broeckx G, et al. Image-based multiplex immune profiling of cancer tissues: translational implications. A report of the International Immunology Biomarker Working Group on Breast Cancer. *J Pathol* 2024;262:271-88.
22. Rojas F, Hernandez S, Lazcano R, et al. Multiplex Immunofluorescence and the Digital Image Analysis Workflow for Evaluation of the Tumor Immune Environment in Translational Research. *Front Oncol* 2022;12:889886.
23. Abdullahi Sidi F, Bingham V, Craig SG, et al. PD-L1 Multiplex and Quantitative Image Analysis for Molecular Diagnostics. *Cancers (Basel)* 2020;13:29.
24. Wu F, Jiang T, Chen G, et al. Multiplexed imaging of tumor immune microenvironmental markers in locally advanced or metastatic non-small-cell lung cancer characterizes the features of response to PD-1 blockade plus chemotherapy. *Cancer Commun (Lond)* 2022;42:1331-46.
25. Li C, Hu M, Cai S, et al. Dysfunction of CD8(+) T cells around tumor cells leads to occult lymph node metastasis in NSCLC patients. *Cancer Sci* 2024;115:2528-39.
26. Yang L, Zhang W, Sun J, et al. The role of spatial interplay patterns between PD-L1-positive tumor cell and T cell in recurrence of locally advanced non-small cell lung cancer. *Cancer Immunol Immunother* 2023;72:2015-27.
27. Tan WCC, Nerurkar SN, Cai HY, et al. Overview of multiplex immunohistochemistry/immunofluorescence techniques in the era of cancer immunotherapy. *Cancer Commun (Lond)* 2020;40:135-53.
28. Inoue C, Miki Y, Saito R, et al. PD-L1 Induction by Cancer-Associated Fibroblast-Derived Factors in Lung Adenocarcinoma Cells. *Cancers (Basel)* 2019;11:1257.
29. Zheng X, Weigert A, Reu S, et al. Spatial Density and Distribution of Tumor-Associated Macrophages Predict Survival in Non-Small Cell Lung Carcinoma. *Cancer Res* 2020;80:4414-25.
30. Yang L, Zhang W, Sun J, et al. Functional status and spatial interaction of T cell subsets driven by specific tumor microenvironment correlate with recurrence of non-small cell lung cancer. *Front Immunol* 2022;13:1022638.
31. Cai S, Yang G, Hu M, et al. Spatial cell interplay networks of regulatory T cells predict recurrence in patients with operable non-small cell lung cancer. *Cancer Immunol Immunother* 2024;73:189.

32. Lopez de Rodas M, Wang Y, Peng G, et al. Objective Analysis and Clinical Significance of the Spatial Tumor-Infiltrating Lymphocyte Patterns in Non-Small Cell Lung Cancer. *Clin Cancer Res* 2024;30:998-1008.
33. Hakoziaki T. Quantitative spatial profiling of PD-1/PD-L1 interaction in patients with cancer. *Transl Lung Cancer Res* 2023;12:1346-9.
34. Liu W, Chen C, Li C, et al. Comprehensive Analysis of Immune Responses to Neoadjuvant Immunotherapy in Resectable Non-small Cell Lung Cancer. *Ann Surg Oncol* 2024;31:9332-43.
35. Guo W, Qiao T, Li H, et al. Peripheral CD8(+) PD-1(+) T cells as novel biomarker for neoadjuvant chemioimmunotherapy in humanized mice of non-small cell lung cancer. *Cancer Lett* 2024;597:217073.
36. Caushi JX, Zhang J, Ji Z, et al. Transcriptional programs of neoantigen-specific TIL in anti-PD-1-treated lung cancers. *Nature* 2021;596:126-32.
37. Cascone T, Leung CH, Weissferdt A, et al. Neoadjuvant chemotherapy plus nivolumab with or without ipilimumab in operable non-small cell lung cancer: the phase 2 platform NEOSTAR trial. *Nat Med* 2023;29:593-604.
38. Mellman I, Chen DS, Powles T, et al. The cancer-immunity cycle: Indication, genotype, and immunotype. *Immunity* 2023;56:2188-205.
39. Rudolf J, Büttner-Herold M, Erlenbach-Wünsch K, et al. Regulatory T cells and cytotoxic T cells close to the epithelial-stromal interface are associated with a favorable prognosis. *Oncoimmunology* 2020;9:1746149.
40. Lopez de Rodas M, Nagineni V, Ravi A, et al. Role of tumor infiltrating lymphocytes and spatial immune heterogeneity in sensitivity to PD-1 axis blockers in non-small cell lung cancer. *J Immunother Cancer* 2022;10:e004440.
41. Mendiola M, Pellinen T, Ramon-Patino JL, et al. Prognostic implications of tumor-infiltrating T cells in early-stage endometrial cancer. *Mod Pathol* 2022;35:256-65.
42. Donnem T, Hald SM, Paulsen EE, et al. Stromal CD8+ T-cell Density—A Promising Supplement to TNM Staging in Non-Small Cell Lung Cancer. *Clin Cancer Res* 2015;21:2635-43.
43. Liu Q, Ou Q, Shen L, et al. BATF Potentially Mediates Negative Regulation of PD-1/PD-Ls Pathway on T Cell Functions in Mycobacterium tuberculosis Infection. *Front Immunol* 2019;10:2430.
44. Wang B, Zhou B, Chen J, et al. Type III interferon inhibits bladder cancer progression by reprogramming macrophage-mediated phagocytosis and orchestrating effective immune responses. *J Immunother Cancer* 2024;12:e007808.
45. Śledzińska A, Vila de Mucha M, Bergerhoff K, et al. Regulatory T Cells Restrain Interleukin-2- and Blimp-1-Dependent Acquisition of Cytotoxic Function by CD4(+) T Cells. *Immunity* 2020;52:151-166.e6.
46. Sánchez-Magraner L, Miles J, Baker CL, et al. High PD-1/PD-L1 Checkpoint Interaction Infers Tumor Selection and Therapeutic Sensitivity to Anti-PD-1/PD-L1 Treatment. *Cancer Res* 2020;80:4244-57.
47. Balança CC, Salvioni A, Scarlata CM, et al. PD-1 blockade restores helper activity of tumor-infiltrating, exhausted PD-1hiCD39+ CD4 T cells. *JCI Insight* 2021;6:e142513.
48. Mosteiro A, Pedrosa L, Ferrés A, et al. The Vascular Microenvironment in Glioblastoma: A Comprehensive Review. *Biomedicines* 2022;10:1285.
49. Lamplugh Z, Fan Y. Vascular Microenvironment, Tumor Immunity and Immunotherapy. *Front Immunol* 2021;12:811485.
50. Bach VN, Ding J, Yeung M, et al. A Negative Regulatory Role for RKIP in Breast Cancer Immune Response. *Cancers (Basel)* 2022;14:3605.
51. Schenkel JM, Pauken KE. Localization, tissue biology and T cell state - implications for cancer immunotherapy. *Nat Rev Immunol* 2023;23:807-23.
52. Mills KHG. IL-17 and IL-17-producing cells in protection versus pathology. *Nat Rev Immunol* 2023;23:38-54.

Cite this article as: Yang L, Geng J, Yang H, Zhao M, Yuan H, Yan Y, Wu L, Cao F, Xing L, Sun X. Closer proximity of pre-treatment CD4⁺ T cells to CD8⁺ T cells favor response to neoadjuvant immunotherapy in patients with PD-L1 low-expressing non-small cell lung cancer. *Transl Lung Cancer Res* 2025;14(3):810-823. doi: 10.21037/tlcr-24-886